

Remarkable Functions of Long-Chain Alkyl Groups in Halogen-Bridged Nickel(III) Nanowire Complexes

Hideki Ohtsu,^{*,[a]} Shinya Takaishi,^[b] Keita Imamura,^[b] Ayumi Ishii,^[a] Koji Tanaka,^[c] Miki Hasegawa,^[a] and Masahiro Yamashita^{*,[b]}

Keywords: Nickel / Nanostructures / Long-chain alkyl groups / Average-valent compounds / Thin films

The long-chain alkyl groups of new bidentate ligands make it possible to generate nickel MX-chain complexes exhibiting the shortest Ni^{III}–Ni^{III} distance among all MX-chain compounds reported. Dissolution in organic solvents occurs with-

out dissociation of the MX-chain units, and the successful fabrication of thin films is reported.

(© Wiley-VCH Verlag GmbH & Co. KGaA, 69451 Weinheim, Germany, 2007)

Introduction

Much attention has been paid to quasi-one-dimensional assembled electronic systems in the fields of chemistry and physics because these compounds exhibit novel phenomena such as the generation of solitons and polarons in π -conjugated polymers,^[1,2] metallic^[3] and super-conductivity,^[4] and slow magnetic relaxation in several ferromagnetic and ferrimagnetic complexes.^[5] Among such one-dimensional compounds, halogen-bridged quasi-one-dimensional transition-metal complexes (MX-chain complexes) have been one of the most important and attractive research objectives, as they exhibit various electronic states and many noticeable physical properties such as intense charge-transfer bands,^[6] overtone progressions of the resonance Raman spectra,^[7] intense luminescence spectra with large Stokes shifts,^[8] photogeneration^[9] and long-range migration^[10] of solitons and polarons, and gigantic third-order optical nonlinearity,^[11] etc.

The electronic structures of MX-chain compounds have been regarded as extended Peierls–Hubbard models,^[12]

where the electron–phonon interaction (S), electron transfer (T), and intra- and intersite Coulomb repulsion energies (U and V , respectively) compete or cooperate with each other. Pt and Pd compounds indicate charge-density-wave (CDW) states caused by the strong S , where the bridging halide ions are displaced from the midpoints between the neighboring two metal ions ($\cdots M^{II}\cdots X-M^{IV}-X\cdots M^{II}\cdots X-M^{IV}-X\cdots$).^[13,14] On the other hand, Ni compounds are Mott–Hubbard-type MX-chain complexes induced by the strong U , where the bridging halide ions are located at the midpoints between the neighboring two metal ions ($-M^{III}-X-M^{III}-X-M^{III}-X-M^{III}-X-$).^[13,15]

A number of MX-chain complexes have so far been synthesized and characterized to provide further valuable insight into the characteristic electronic structures and unique physical properties. In particular, the MX-chain complex $[Ni^{III}(chxn)_2Br]Br_2$ ^[16] has been attracting much attention because it shows the largest gigantic third-order optical nonlinearity [$\chi^{(3)} = \text{ca. } 10^{-4} \text{ esu}$].^[11] The special feature of this compound, however, appears only in the solid state, as MX-chain units are disrupted in solution. The inherent instability of the complex in solution has precluded further development into useful molecular devices such as thin films.

Reported herein is the synthesis and characterization of nickel MX-chain complexes supported by new bidentate ligands with long-chain alkyl groups (Figure 1) that not only impart solubility to the MX-chain compounds but these groups also cause the shortening of the M–M distances, which can result in increased $\chi^{(3)}$ values.^[11] Moreover, we attained the successful fabrication of thin films consisting of the MX-chain complexes, which can be promising candidates for optical switching devices.

[a] Department of Chemistry and Biological Science, College of Science and Engineering, Aoyama Gakuin University
5-10-1 Fuchinobe, Sagami-hara 229-8558, Japan
Fax: +81-42-759-6493
E-mail: ohtsu@chem.aoyama.ac.jp

[b] Department of Chemistry, Graduate School of Science, Tohoku University and CREST (JST)
6-3 Aramaki Aza-Aoba, Aoba-ku, Sendai 980-8578, Japan
Fax: +81-22-795-6544
E-mail: yamasita@agnus.chem.tohoku.ac.jp

[c] Institute for Molecular Science
5-1, Higashiyama, Myodaiji, Okazaki 444-8787, Japan
Supporting information for this article is available on the WWW under <http://www.eurjic.org> or from the author.

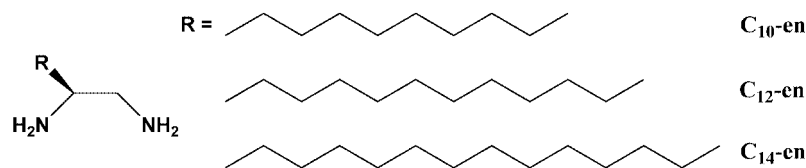


Figure 1. Structures of bidentate ligands having long-chain alkyl groups.

Results and Discussion

The nickel MX-chain complexes, represented as $[Ni^{III}-(C_n\text{-en})_2Br]Br_2$ [$n = 10$ (**1**), 12 (**2**), and 14 (**3**)], were obtained as black microcrystals by puffing Br_2 gas into the corresponding nickel(II) complexes in ethanol, and the compositions of **1**, **2**, and **3** were determined by elemental analysis. The syntheses of these complexes afforded no well-shaped single crystals; however, we successfully obtained accurate powder X-ray diffraction (XRD) data for **1**, **2**, and **3** by synchrotron powder diffraction with a large Debye-Scherrer camera at 100 K and are able to image the XRD data for **3** by the Rietveld method as shown in Figure 2.^[17,18]

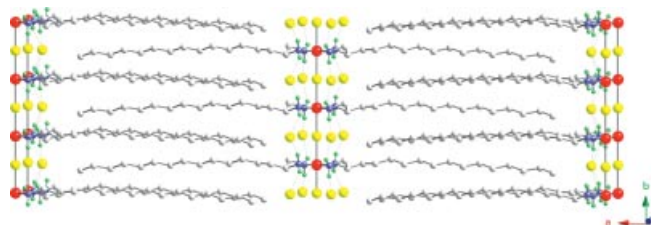


Figure 2. Representation of the molecular structure of **3** on the basis of the results of synchrotron XRD, IR, and EPR measurements (Ni red, Br yellow, C gray, H green, N blue).

Ni^{III} ions and bromide ions are arranged alternately along the b axis to form the linear MX-chain structures. The linear chains are connected by hydrogen bonds between the hydrogen atoms of the amino group of the $C_{14}\text{-en}$ ligand and the counter bromide ions, which is consistent with an IR spectrum exhibiting a signal due to the hydrogen-bonded N–H stretching mode of the ligand at 3005 cm^{-1} (Figure S2).^[19] The bridging bromide ions are placed at the midpoints between the neighboring two nickel ions, a fact that indicates the electronic structure of **3** is a Mott–Hubbard state, and the assignment of which is harmonic with the results of IR spectroscopy (Figure S2)^[20] and temperature-dependent EPR measurements (Figure S3).^[21] In the case of **1** and **2**, these molecular structures and electronic configurations are essentially the same as those of **3** except for the length of the alkyl chain of the bidentate ligands, and the structures are strongly supported by synchrotron XRD, IR, and EPR studies. It should be noted that the $Ni^{III}\text{--}Ni^{III}$ distance (5.06 \AA) in all the complexes is the shortest among all of the MX-chain complexes reported so far $\{[Ni^{III}(\text{chxn})_2Br]Br_2\ 5.157(1)\text{ \AA}$,^[15,16] $[Ni^{III}(\text{bn})_2Br]Br_2\ 5.136(6)\text{ \AA}$,^[22,23] $[Ni^{III}(\text{pn})_2Br]Br_2\ 5.110(7)\text{ \AA}$ ^[22,24]. Such a drastic shortening in the $Ni^{III}\text{--}Ni^{III}$ distance may be ascribed to the chemical pressure effect induced by the hydro-

phobic interaction between the long-chain alkyl groups of the bidentate ligands.

The function of the long-chain alkyl groups *cannot* confine itself to leading the chemical pressure effect. These groups of the ligands enable us to disperse the nickel MX-chain complexes in organic solvents without the decomposition of MX-chain cores and to fabricate thin films containing the MX-chain compounds. Figure 3 displays the absorption spectrum of **3** in chloroform solution and as a thin film together with that in the solid state at 298 K. The intense absorption band centered at 1.33 eV is observed in solution and as a thin film and is quite the same as that in the solid state.^[25] This characteristic absorption band can be assigned to the charge-transfer band from the bridging bromide ion to the upper Hubbard band of the nickel $3d_{z^2}$ orbital along the MX-chain direction.^[12] In addition, it should be noted that no absorption spectral disturbance caused by light scatterings is observed even in the higher energy region. In fact, the size of **3** ($0.1\text{--}0.7\text{ }\mu\text{m}$) as determined by scanning electron microscopy (SEM) is much smaller than the wavelength in the visible light region (Figure S5); the morphology and height distributions of the thin films characterized by using atomic force microscopy (AFM) analysis are quite smooth and $1.54 \pm 0.03\text{ }\mu\text{m}$ in thickness (Figure S6). The lack of interruption due to light scatterings can thus be the reason why nickel MX-chain complex **3** is dispersed uniformly in solution and as a thin film with the help of the long-chain alkyl groups.^[26]

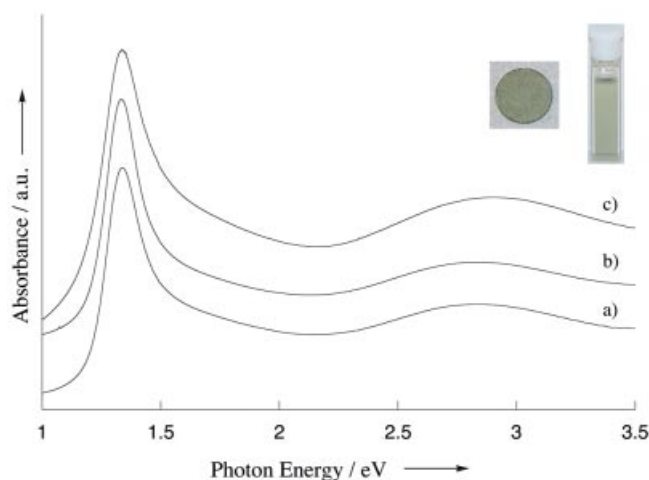


Figure 3. Absorption spectra of **3** in (a) chloroform solution, (b) film state, and (c) solid state at 298 K. Inset: Photographs of **3** (right) in solution and (left) as a thin film.

Conclusions

We successfully synthesized nickel MX-chain complexes exhibiting not only the shortest Ni^{III}–Ni^{III} distance among all MX-chain compounds reported. The solubility of these compounds in organic solvents occurs without dissociation of the MX-chain units bearing new bidentate ligands containing the long-chain alkyl groups. Moreover, the successful fabrication of thin films consisting of the nickel nanowire complex has been accomplished by the spin-coating method. These results provide valuable information for the further development of MX-chain complexes having many interesting physical properties derived from one-dimensional electronic systems and shed light on the applications of functional transition-metal complexes.

Experimental Section

Materials: All chemicals used for the synthesis of the ligands and complexes were commercial products of the highest available purity and were further purified by standard methods.^[27] Solvents were also purified by standard methods before use.^[27]

Synthesis: All ligands and complexes used in this study were prepared according to the following procedures, and the structures of the products were confirmed by analytical data (vide infra).

(S)-Dodecane-1,2-diamine (C_{10-en}), (S)-Tetradecane-1,2-diamine (C_{12-en}), and (S)-Hexadecane-1,2-diamine (C_{14-en}): These ligands were synthesized by a literature procedure.^[28,29]

[Ni^{II}(C_{10-en})₂Br₂]: To a methanol solution of C_{10-en} (1.002 g, 5.0 mmol) was added NiBr₂·3H₂O (0.681 g, 2.5 mmol) in methanol. Addition of ether to the resulting solution gradually gave pale violet powder that was collected by filtration and recrystallized from ethanol. Yield: 0.628 g (40.5%). C₂₄H₅₆Br₂N₄Ni (619.25): calcd. C 46.55, H 9.11, N 9.04; found C 46.25, H 9.05, N 9.17.

[Ni^{II}(C_{12-en})₂Br₂]: This complex was prepared in the same manner as that for the synthesis of [Ni^{II}(C_{10-en})₂Br₂] by using the C_{12-en} ligand instead of C_{10-en}. Yield: 1.016 g (60.2%). C₂₈H₆₄Br₂N₄Ni (675.36): calcd. C 49.79, H 9.55, N 8.29; found C 49.34, H 9.02, N 8.28.

[Ni^{II}(C_{14-en})₂Br₂]: This complex was prepared in the same manner as that for the synthesis of [Ni^{II}(C_{10-en})₂Br₂] by using the C_{14-en} ligand instead of C_{10-en}. Yield: 1.245 g (68.1%). C₃₂H₇₂Br₂N₄Ni (731.47): calcd. C 52.54, H 9.92, N 7.65; found C 52.12, H 9.62, N 7.62.

[Ni^{III}(C_{10-en})₂Br][Br₂ (1): Br₂ gas was puffed in a ethanol suspension of [Ni^{II}(C_{10-en})₂Br₂] (0.062 g, 0.1 mmol). Black powder immediately precipitated and was separated by filtration. Yield: 0.056 g (80.7%). C₂₄H₅₇Br₃N₄NiO_{0.5} (708.16): calcd. C 40.70, H 8.11, N 7.91; found C 40.79, H 7.94, N 7.96.

[Ni^{III}(C_{12-en})₂Br][Br₂ (2): This complex was prepared in the same manner as that for the synthesis of [Ni^{III}(C_{10-en})₂Br][Br₂] by using [Ni^{II}(C_{12-en})₂Br₂] instead of [Ni^{II}(C_{10-en})₂Br₂]. Yield: 0.073 g (96.0%). C₂₈H₆₆Br₃N₄NiO (773.28): calcd. C 43.49, H 8.60, N 7.24; found C 43.32, H 8.25, N 7.25.

[Ni^{III}(C_{14-en})₂Br][Br₂ (3): This complex was prepared in the same manner as that for the synthesis of [Ni^{III}(C_{10-en})₂Br][Br₂] by using [Ni^{II}(C_{14-en})₂Br₂] instead of [Ni^{II}(C_{10-en})₂Br₂]. Yield: 0.081 g (99.6%). C₂₄H₅₆Br₂N₄Ni (619.25): calcd. C 46.34, H 8.99, N 6.75; found C 46.00, H 8.55, N 6.75.

Fabrication of the Thin Films of 3: Compound 3 (10.0 mg) was dispersed in chloroform (0.5 mL) containing PMMA (36.5 mg) with ultrasonication, and the resulting dispersion was filtered through a 1.0-μm membrane filter. The thin films were prepared from the blend solution by spin-coating on quartz substrates (φ = 10 mm).

Measurements: Synchrotron XRD measurements were carried out with a SPring-8 BL02B2 beam line to obtain XRD data with high angular resolution (2θ = 1–75°) at 100 K. The sample powders were sufficiently fine and gave a homogeneous intensity distribution in the Debye–Scherrer powder ring. The powder samples were enclosed in silica glass capillaries (0.3 mm internal diameter). The exposure time was 40 min, and reflections were collected on an imaging plate installed on a large Debye–Scherrer camera. The wavelength of the incident X-rays was ≈ 1.0 Å, which was calibrated by using standard CeO₂ powder. The structure was solved by the Rietveld technique, and the hydrogen atoms of the NH₂ group were located at the calculated positions. Infrared spectra were measured as KBr disks with a JASCO FTIR-620 spectrophotometer. EPR spectra were taken with a JEOL JES-FA200 equipped with an attached VT (Variable Temperature) apparatus and were recorded under nonsaturating microwave power conditions. The magnitude of the modulation was chosen to optimize the resolution and the signal-to-noise ratio of the observed spectra. The g values were calibrated with a Mn^{II} marker used as a reference. Electronic absorption spectra were recorded with a Shimadzu UV-3100PC spectrophotometer with the samples prepared as KBr pellets in the case of the solid states. SEM measurements were performed with a JEOL JSM-6390LA operated at an accelerating voltage of 1.5 kV. Samples for SEM studies were prepared by placing a drop of the chloroform dispersion of the nanowire complexes on a piece of Pt plate under ambient conditions; the sample was then dried and stored in vacuo for SEM characterization. AFM imaging was carried out in noncontact mode with a JEOL JSPM-5200. Elemental analyses were carried out at the Research and Analytical Center for Giant Molecules, Graduate School of Science, Tohoku University.

Supporting Information (see footnote on the first page of this article): XRD, IR, EPR, absorption spectra, SEM, and AFM data.

Acknowledgments

The synchrotron radiation X-ray powder diffraction experiments were performed at Spring-8 BL02B2 with the approval of the Japan Synchrotron Radiation Research Institute (JASRI) (proposal no. 2006A1646). We are grateful to Dr. Keiichi Osaka, Dr. Kenichi Kato, and Prof. Masaki Takata for helpful experiments at JASRI and to Dr. Eiji Nishibori, Prof. Masaki Takata, and Prof. Makoto Sakata for permitting the use of their Rietveld program. We also thank JEOL Ltd. for SEM measurements. This work was partly supported by a grant from the Aoyama Gakuin 21st Century COE Program and supported in part by a Grant-in-Aid for Scientific Research on Priority Areas (Chemistry of Coordination Space) from the Ministry of Education, Culture, Sports, Science, and Technology.

- [1] I. B. Goldberg, H. R. Crowe, P. R. Newman, A. J. Heeger, A. G. MacDiarmid, *J. Chem. Phys.* **1979**, *70*, 1132–1136.
- [2] W. P. Su, J. R. Schrieffer, A. J. Heeger, *Phys. Rev. B* **1980**, *22*, 2099–2111.
- [3] a) H. Yersin, G. Gliemann, *Ann. N. Y. Acad. Sci.* **1978**, *313*, 539–559; b) J. S. Miller (Ed.), *Extended Linear Chain Compounds, Vols. 1–3*, Plenum, New York, **1982**.
- [4] a) J. G. Bednorz, K. A. Mueller, *Z. Phys.* **1986**, *64*, 189–193; b) M. K. Wu, J. R. Ashburn, C. J. Torng, P. H. Hor, R. L. Meng,

- L. Gao, Z. J. Huang, Y. Q. Wanag, C. W. Chu, *Phys. Rev. Lett.* **1987**, 58, 908–910.
- [5] a) A. Caneschi, D. Gatteschi, N. Lalioti, C. Sangregorio, R. Sessoli, G. Venturi, A. Vindigni, A. Rettori, M. G. Pini, M. A. Novak, *Angew. Chem.* **2001**, 113, 1810–1813; *Angew. Chem. Int. Ed.* **2001**, 40, 1760–1763; b) R. Clérac, H. Miyasaka, M. Yamashita, C. Coulon, *J. Am. Chem. Soc.* **2002**, 124, 12837–12844; c) R. Lescouëzec, J. Vaissermann, C. Ruiz-Pérez, F. Lloret, R. Carrasco, M. Julve, M. Verdaguer, Y. Dromzee, D. Gatteschi, W. Wernsdorfer, *Angew. Chem.* **2003**, 115, 1521–1524; *Angew. Chem. Int. Ed.* **2003**, 42, 1483–1486.
- [6] a) M. Tanaka, S. Kurita, T. Kojima, Y. Yamada, *Chem. Phys. Lett.* **1984**, 91, 257–265; b) Y. Wada, T. Mitani, M. Yamashita, T. Koda, *J. Phys. Soc. Jpn.* **1985**, 54, 3143–3153.
- [7] a) R. J. H. Clark, M. L. Franks, W. R. Trumble, *Chem. Phys. Lett.* **1976**, 41, 287–292; b) R. J. H. Clark, M. Kurmoo, D. N. Mountney, H. Toftlund, *J. Chem. Soc. Dalton Trans.* **1982**, 1851–1860; c) R. J. H. Clark, *Adv. Infrared Raman Spectrosc.* **1983**, 11, 95–130.
- [8] H. Tanino, K. Kobayashi, *J. Phys. Soc. Jpn.* **1983**, 52, 1446–1456.
- [9] H. Okamoto, T. Mitani, K. Toriumi, M. Yamashita, *Phys. Rev. Lett.* **1992**, 69, 2248–2251.
- [10] N. Kimura, S. Ishimaru, R. Ikeda, M. Yamashita, *J. Chem. Soc. Faraday Trans.* **1998**, 94, 3659–3663.
- [11] H. Kishida, H. Matsuzaki, H. Okamoto, T. Manabe, M. Yamashita, Y. Taguchi, Y. Tokura, *Nature* **2000**, 405, 929–932.
- [12] H. Okamoto, Y. Shimada, Y. Oka, A. Chainani, T. Takahashi, H. Kitagawa, T. Mitani, K. Toriumi, K. Inoue, T. Manabe, M. Yamashita, *Phys. Rev. B* **1996**, 54, 8438–8445.
- [13] M. B. Robin, P. Day, *Adv. Inorg. Chem. Radiochem.* **1967**, 10, 247–422.
- [14] A. Hazell, *Acta Crystallogr., Sect. C* **1991**, 47, 962–966.
- [15] K. Toriumi, Y. Wada, T. Mitani, S. Bandow, M. Yamashita, Y. Fujii, *J. Am. Chem. Soc.* **1989**, 111, 2341–2342.
- [16] chxn = (1*R*,2*R*)-diaminocyclohexane.
- [17] The reliability factors based on the powder pattern (R_{wp}) and the Bragg integrated intensities (R_I) were 8.78 and 11.7%, respectively. Observed and calculated synchrotron X-ray powder diffraction patterns and the determined unit cell parameters are given in Figure S1 and Table S1, respectively.
- [18] Only one orientation of the disordered long-chain alkyl group is shown for the sake of clarity.
- [19] IR measurements around 3000 cm⁻¹ are good probes for elucidating the electronic states of the MX-chain complexes. A Mott–Hubbard state shows a singlet $\nu(N-H)$ signal, whereas a CDW state exhibits a double $\nu(N-H)$ signal; see ref.^[20]
- [20] K. Okaniwa, H. Okamoto, T. Mitani, K. Toriumi, M. Yamashita, *J. Phys. Soc. Jpn.* **1991**, 60, 997–1004.
- [21] H. Okamoto, K. Toriumi, T. Mitani, M. Yamashita, *Phys. Rev. B* **1990**, 42, 10381–10387.
- [22] M. Sasaki, S. Takaishi, H. Miyasaka, K. Sugiura, M. Yamashita, *J. Am. Chem. Soc.* **2005**, 127, 14958–14959.
- [23] bn = (2*R*,3*R*)-diaminobutane.
- [24] pn = (*R*)-1,2-diaminopropane.
- [25] The same absorption bands are observed in the case of **1** (1.33 eV) and **2** (1.33 eV); see Figure S4.
- [26] a) N. Kimizuka, N. Oda, T. Kunitake, *Inorg. Chem.* **2000**, 39, 2684–2689; b) N. Kimizuka, S. H. Lee, T. Kunitake, *Angew. Chem.* **2000**, 112, 402–404; *Angew. Chem. Int. Ed.* **2000**, 39, 389–391; c) N. Kimizuka, *Adv. Mater.* **2000**, 12, 1461–1463.
- [27] D. D. Perrin, W. L. F. Armarego, *Purification of Laboratory Chemicals*, Butterworth–Heinemann, Oxford, **1988**.
- [28] L. He, H.-S. Byun, R. Bittman, *J. Org. Chem.* **2000**, 65, 7618–7626.
- [29] S. G. Gouin, J. F. Gustin, K. Joly, A. Loussouarn, A. Reliquet, J. C. Meslin, D. Deniaud, *Tetrahedron* **2002**, 58, 1131–1136.

Received: July 19, 2007

Published Online: August 28, 2007